ARTICLE

Photodissociation of HOD via the $\widetilde{C}^1B_1$ State: OD/OH Branching Ratio and OD Bond Dissociation Energy

Li-na Cheng, Yuan Cheng, Kai-jun Yuan*, Qing Guo, Tao Wang, Dong-xu Dai, Xue-ming Yang*

State key Laboratory of Molecular Reaction Dynamics, Dalian Institute of Chemical Physics, Chinese Academy of Sciences, Dalian 116023, China

(Dated: Received on October 6, 2010; Accepted on November 3, 2010)

Photodissociation of jet-cooled HOD via the $\widetilde{C}$ state around 124 nm has been studied using the H(D)-atom Rydberg tagging time-of-flight technique. Rotational state resolved action spectrum and the product translational energy distribution spectra have been recorded for both D+OH and H+OD dissociation channels. Product channel OH/OD branching ratios for the individual $\widetilde{C}$-$\widetilde{X}$ rotational transition have been determined. A comparison is also given with the $\widetilde{B}$-$\widetilde{X}$ and $\widetilde{A}$-$\widetilde{X}$ transitions. In addition, the dissociation energy of the OD bond in HOD has been determined accurately to be 41751.3±5 cm^{-1}.

Key words: Photodissociation, Rydberg tagging, Branching ratio, Dissociation energy

I. INTRODUCTION

Photodissociation of water molecules in the vacuum ultraviolet (VUV) region is important in atmospheric chemistry and interstellar chemistry, and has been the subject of extensive experimental and theoretical studies over several decades [1, 2]. Interesting photodissociaton dynamics of several electronic states, $\widetilde{X}^1A_1$, $\widetilde{A}^1B_1$, $\widetilde{B}^1A_1$, $\widetilde{C}^1B_1$, and $\widetilde{D}^1A_1$, have been revealed. These electronic states were found to be strongly coupled to each other. Excitation of the water molecule to the lowest excited state, $\widetilde{A}^1B_1$, results in a direct dissociation that produces an H atom plus a ground state OH($X^2\Pi$) radical [3−5]. For dissociation of water via the $\widetilde{B}^1A_1$ state, the OH products in the $A^2\Sigma^+$ state as well as in the $X^2\Pi$ state, with extremely high rotational excitation, are produced. The OH($X^2\Pi$) product channel occurs via two non-adiabatic dissociation pathways from the $\widetilde{B}$ state: Renner-Teller coupling to $\widetilde{A}^1B_1$ and conical intersections between $\widetilde{B}^1A_1$ and $\widetilde{X}^1A_1$ [6−10]. For dissociation via the $\widetilde{D}^1A_1$ state, the water molecule breaks up via a fast predissociation mechanism due to the strong nonadiabatic coupling to the $\widetilde{B}^1A_1$ state [11]. All these three excited electronic states have very short lifetimes in the range of ten femtoseconds. The absorption spectra of these states all show broad continua in the VUV region.

The absorption spectrum of the $\widetilde{C}^1B_1$←$\widetilde{X}^1A_1$ transition peaked at 124 nm, however, consists of several sharp peaks that can be assigned to individual rotational transitions. The experimentally measured linewidths of these transitions suggest that the $\widetilde{C}^1B_1$ state has a lifetime (a few picoseconds) that is roughly two orders of magnitude longer than that of the nearby three excited electronic states. This suggests that the coupling of the $\widetilde{C}^1B_1$ state to other states are much weaker than the $\widetilde{B}$ and $\widetilde{D}$ electronic states. Photodissociation of the $\widetilde{C}^1B_1$ state has also served as the model system for studying the rotational state specific photodissociation. Two distinctive predissociation mechanisms, homogeneous and heterogeneous dissociation mechanisms, have been indicated previously by resonance enhanced multiphoton ionization (REMPI) studies [12, 13]. Recently, the rotational state specific photodissociation dynamics of the $\widetilde{C}^1B_1$ state of the H_2O molecule have been studied in our laboratory, using the sensitive H-atom Rydberg tagging technique, in combination with a strong tunable VUV light source [14]. These results indicate that the photodissociation process occurs exclusively through a homogeneous nonadiabatic coupling to the $\widetilde{A}^1B_1$ state for H_2O in rotational states with k'_a=0, leading to rotationally cold and vibrationally hot OH(X) products (up to v=13). In contrast, for H_2O in rotationally excited states with k'_a>0, an additional heterogeneous dissociation pathway opens via Coriolis-type coupling to the $\widetilde{B}^1A_1$ state surface. This yields extremely rotationally hot and vibrationally cold ground state OH(X) and electronically excited OH(A) products.

Recently, the HOD photodissociation via the same $\widetilde{C}^1B_1$ state has also been investigated [15]. The action spectrum of the $\widetilde{C}^1B_1$←$\widetilde{X}^1A_1$ band has also been obtained [15]. The rotational oscillations in product OH(X) and OD(X) population, most striking for the OH case, were attributed to the symmetry properties

*Authors to whom correspondence should be addressed. E-mail: xmyang@dicp.ac.cn, kjyuan@dicp.ac.cn

of the product rotational wavefunctions around the coupling angle of 90° accompanying non-adiabatic transfer from the $\widetilde{C}$ state to the $\widetilde{A}$ state [15]. In addition, we have also carried out the two-photon dissociation studies of H_2O, D_2O, and HOD via the $\widetilde{C}^1B_1$ state, which is a natural extension of our previous water photochemistry studies [16−18].

It is known that vibrationally mediated selective bond photodissociation process leads to variation of branching ratios [19−21], however, few studies have been carried out on the effect of rotational excitation on the branching ratios in molecular photochemistry. In this work, we will present our recent experimental results on the rotational specific HOD photodissociation in the $\widetilde{C}$ state, especially the results of the rotational excitation effect on the branching ratios of the two dissociation channels. In addition, accurate dissociation energy of the OD bond, D_0(D−OH), in HOD has also been determined in this work.

II. EXPERIMENTS

The Rydberg H(D)-atom time-of-flight technique [22, 23], in combination with a tunable VUV laser source developed in our laboratory [24], has been utilized in the study of the photodissociation dynamics of the HOD molecule via the $\widetilde{C}$ state. The experimental scheme used in this work is almost exactly the same as our previous works [14−18]. The HOD sample was prepared by premixing H_2O and D_2O samples with a 1:1 ratio at room temperature, and then expanded together with Ar through a pulsed valve at a stagnation pressure of 80−120 kPa. In the beam, H_2O, HOD and D_2O are also present. The jet-cooled molecular beam was incepted by a tunable VUV photolysis light beam as well as the Rydberg tagging detection laser beams. The VUV photolysis light source around 124 nm as well as 121.6 nm light beam for Lyman α line pumping of the H(D)-atom was generated using the two-photon resonant four-wave mixing scheme in a clean gas cell filled with Krypton gas (about 0.8 kPa) [25]. In the photodissociation region, the product H(D) atoms were then detected by the H(D)-atom Rydberg "tagging" technique in which the H(D) atoms were excited from the ground state to a high Rydberg state via a two-step efficient excitation scheme: the VUV laser (about 121.6 nm) pumps the H(D) atoms from n=1 to n=2, and the UV laser (about 365 nm) then excites them from n=2 to the high Rydberg state (n=30−80). The Rydberg tagged H(D) atoms, after flying a certain distance, were detected by a Z-stack microchannel plate (MCP) detector. The signals were counted by a multi-channel scaler (MCS) system. Since the detection laser 121.6 nm can also generate H(D) signals, background subtraction was made by alternating the VUV photolysis laser on and off. Background signals by 121.6 nm were suppressed so that they were maintained at about ten times smaller than the tunable VUV photolysis signals from HOD.

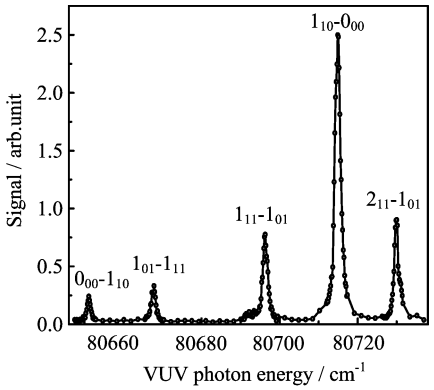

FIG. 1 The action spectrum of the $\widetilde{C}$-$\widetilde{X}$ transition band for HOD near 124 nm. This figure is adapted from Ref.[15].

III. RESULTS AND DISCUSSION

The action spectrum for the $\widetilde{C}$-$\widetilde{X}$ absorption band around 124 nm from photodissociation of HOD is shown in Fig.1, which is adapted from Ref.[15]. According to the transition selection rules, the rotational transitions can be assigned as $J'_{k'_a k'_c}(\widetilde{C}(000))\leftarrow J''_{k''_a k''_c}(\widetilde{X}(000))$. In this action spectrum, five clearly resolved rotational lines at 80650.8, 80667.8, 80696.1, 80713.6, and 80728.1 cm^{-1} are labeled as 0_{00}-1_{10}, 1_{01}-1_{11}, 1_{11}-1_{01}, 1_{10}-0_{00}, and 2_{11}-1_{01}, respectively. For each of the rotational transitions, we have measured the H and D products time-of-flight (TOF) spectra. From these TOF spectra, product translational energy distributions are obtained.

Figure 2 shows the total product translational energy distributions via 0_{00}-1_{10} and 1_{10}-0_{00} transitions with both perpendicular and parallel photolysis laser polarizations for the H+OD channel via the $\widetilde{C}^1B_1$ state, while Fig.3 shows the total product translational energy distributions via 0_{00}-1_{10} and 1_{10}-0_{00} transitions with two different photolysis laser polarizations for the D+OH channel via the $\widetilde{C}^1B_1$ state. The observed structures can all be assigned to the OH and OD rovibrational states in the A and X electronic states. The electronic excited OH(A)/OD(A) products are also prominent with the translational energy E_t smaller than 5300 cm^{-1}, while the OH(X)/OD(X) products are located in the spectra with the E_t larger than 5300 cm^{-1}. From these translational energy spectra, one can construct the three dimensional (3D) product contour plots for photodissociation of HOD via all five transitions. Figures 4 and 5 show the 3D product contour plots for the five rotational lines of the HOD $\widetilde{C}$-$\widetilde{X}$ band for both H+OD and D+OH channels. There are two groups in each plot: the inner group corresponds to the levels of the excited $A^2\Sigma^+$ state of OH/OD, and the outer group

DOI:10.1088/1674-0068/24/02/129-133

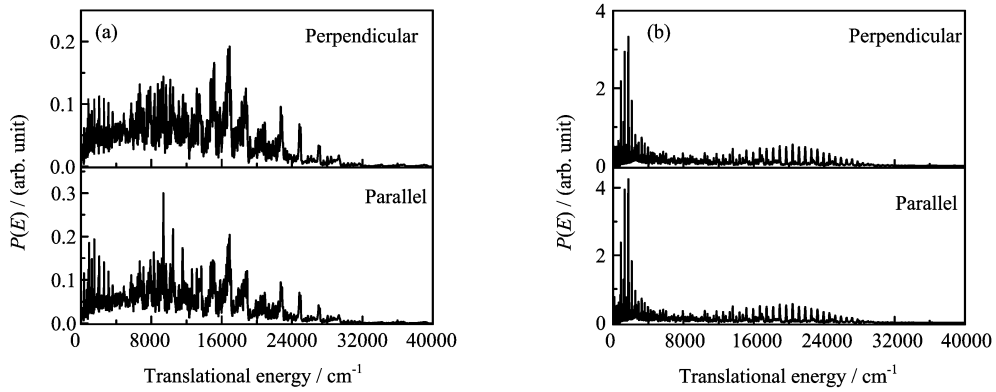

FIG. 2 Total translational energy spectra for the H+OD product channel with the photolysis laser polarization perpendicular and parallel to the detection axis. (a) and (b) correspond to the 0_{00}-1_{10} transition and the 1_{10}-0_{00} transition, respectively.

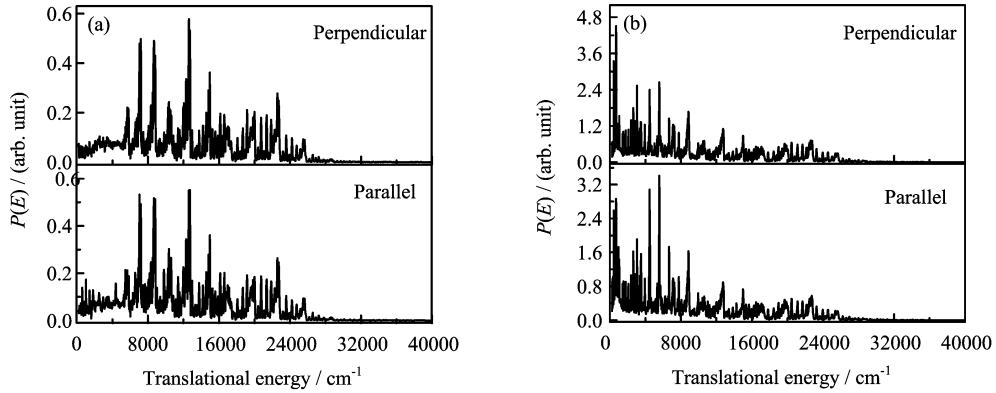

FIG. 3 Total translational energy spectra for the D+OH product channel with the photolysis laser polarization perpendicular and parallel to the detection axis. (a) and (b) correspond to the 0_{00}-1_{10} transition and the 1_{10}-0_{00} transition, respectively.

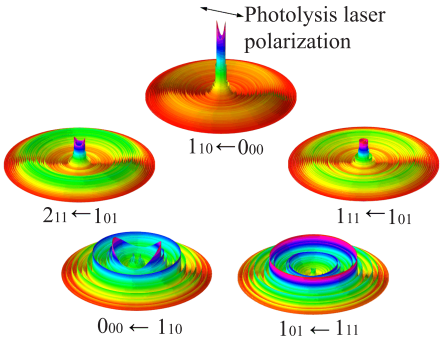

FIG. 4 The 3D product translational energy distribution for the five rotational lines for dissociation to the H+OD channel. The sharp rings correspond to different quantum states of the OD partner product. The inner group of peaks is attributed to the levels of the excited OD($A^2\Sigma$) state, and the outer group of peaks corresponds to the OD($X^2\Pi$) product.

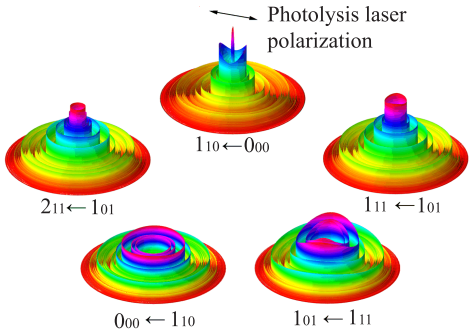

FIG. 5 The 3D product translational energy distribution for the five rotational lines for dissociation to the D+OH channel. The sharp rings correspond to fragmentation different quantum states of the OH partner product. The inner group of peaks is attributed to the levels of the excited OH($A^2\Sigma^+$) state, and the outer group of peaks corresponds to the OH($X^2\Pi$) product.

corresponds to its ground $X^2\Pi$ state.

As mentioned above, photolysis signals and background signals were recorded by alternating the VUV photolysis laser on and off. In order to obtain the accurate branching ratios for H+OD and D+OH channel, the same experimental conditions have been maintained

DOI:10.1088/1674-0068/24/02/129-133

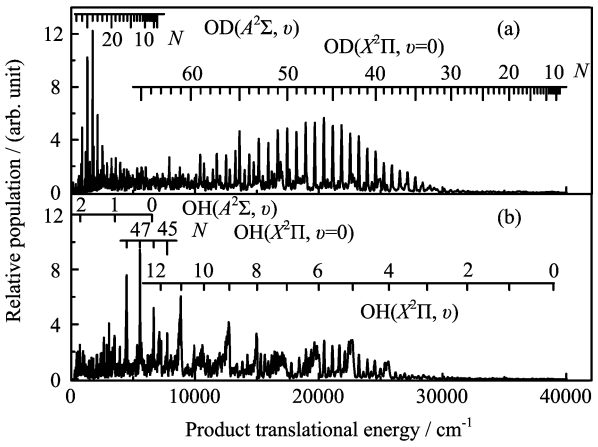

FIG. 6 Total product translational energy distributions for (a) H+OD channel and (b) D+OH channel via the 1_{10}-0_{00} transition at the magic angle 54.7°.

strictly through the whole experimental process. In the experiment, the detection conditions (laser powers *etc.*) are maintained the same for the H and D atom detections. Therefore, the detection efficiency for the H and D atoms should be the same in this experiment. Figure 6 shows the total product translational energy distributions for H+OD channel and D+OH channel of the 1_{10}-0_{00} transition at the magic angle 54.7°. The elementary assignments have been made for OD(X, v=0) and OD(A, v=0) in Fig.6(a), as well as OH(X, v), OH(A, v) and OH(X, v=0) in Fig.6(b). It might be noted that the remarkable rotational states N=45, 46, 47, and 48 for product OH(X, v=0) have been observed from HOD via its $\widetilde{B}$ state at 121.6 nm [9]. However, because of the lower photolysis energies in this experiment, the "super-rotationally" excited states above the dissociation limit of OH($X^2\Pi$) have disappeared [9]. By integrating each rovibrational peak, the quantum yields for both channels can be obtained, thereby their ratio will be considered to be the branching ratio. The branching ratios for $\widetilde{C}$←$\widetilde{X}$ bond of all five rotational transitions 0_{00}-1_{10}, 1_{01}-1_{11}, 1_{11}-1_{01}, 1_{10}-1_{00}, and 2_{11}-1_{01} are 1.31±0.05, 1.15±0.05, 1.10±0.05, 1.28±0.05 and 0.82±0.05, respectively. All these branching ratios are close to the value of 1. This means that the OD+H and OH+D channels are approximately equally populated. Interestingly four branching ratios (OD/OH) of the $\widetilde{C}$←$\widetilde{X}$ rotational transitions are larger than 1, while that of the transition 2_{11}-1_{01} is smaller than 1. This means that the dissociation process of HOD via the $\widetilde{C}^1B_1$ state mostly favors the route to the H+OD channel. It is not immediately clear why the transition 2_{11}-1_{01} shows a different branching ratio from the other four transitions. In previous experimental studies, the branching ratios of the $\widetilde{B}$ and $\widetilde{A}$ state dissociation have been estimated to be 1.66±0.50 [26] and 4±1 [27] or 2.46±15% [4]. Generally, our experimental results are in agreement with the value by Lee and coworkers [26]. The general trend seems in accord with the theoretical prediction that the isotopic branching ratio (OD/OH) is a strong function of the frequency of the dissociation photon [28]. Up to now, full three-dimensional quantum mechanical calculations have been performed only for the $\widetilde{A}$ state dissociation. More accurate theoretical investigations for the upper electronic states are needed in order to understand the dynamical origin of the variation of the branching ratios via different electronic states.

In addition to the branching ratio determination, accurate dissociation energy of the OD bond in the HOD molecule has also been measured. The term values for all the available OH(X) and OH(A) rovibrational levels have been determined accurately from spectroscopic data [7]. In combination with the program designed in our lab, the total product translational energy spectra such as Fig.2 and Fig.3 could be simulated completely. Substantial dynamical results have been obtained from this method [3, 4, 6−11, 14−18]. There is a variable parameter "the available energy of dissociation from the excitation energy of HOD to produce the lowest quantum level of OH($X^2\Pi_{3/2}$, v=0, N=1)", which has been ascertained when the simulated spectra fully identical with the experimental spectra. For the excitation energy of 1_{10}-0_{00} transition, which is known accurately to be 80713.6 cm^{-1}, while the total available energy of dissociation from the 0_{00} level of HOD to produce the lowest quantum level of OH($X^2\Pi_{3/2}$, v=0, N=1) derived from the simulation is 38962.3 cm^{-1}. The dissociation energy D_0^0 defined as from the lowest HOD state to the lowest OH level, is therefore determined to be 41751.3±5 cm^{-1}. Figure 7 shows the energy diagram of the dissociation process of HOD via the $\widetilde{C}$ state for D+OH channel. The error bar on D_0^0 allowed for both statistical and any systematic errors, and should have a confidence at least 95%. This value has been checked out by the other four transitions 0_{00}-1_{10} (about 80650.8 cm^{-1}), 1_{01}-1_{11} (about 80667.8 cm^{-1}), 1_{11}-1_{01} (about 80696.1 cm^{-1}), and 2_{11}-1_{01} (about 80728.1 cm^{-1}), whose initial states for HOD are these excited rotational states $J''_{K''_aK''_c}$ ($\widetilde{X}(000)$)=1_{01}, 1_{10}, and 1_{11} with their respective internal energies as 15.51, 32.52, and 29.82 cm^{-1}.

So far, the most accurate bond dissociation energies for H_2O (about 41151.1±5 cm^{-1}) [7], D_2O (about 41912±20 cm^{-1}) [8], HOD (H+OD channel, about 41283±5 cm^{-1}) [18], and HOD (D+OH channel, about 41751.3±5 cm^{-1}) have all been determined in our laboratory using the high efficiency HRTOF technique. This provides a complete set of the important data of the water molecule and its isotopomers for accurate theoretical investigations.

DOI:10.1088/1674-0068/24/02/129-133

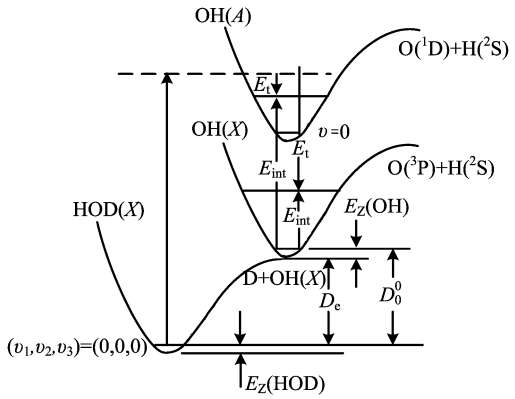

FIG. 7 Energy diagram for the dissociation process of HOD→D+OH via the one-photon dissociation of the $\widetilde{C}$ state.

IV. CONCLUSION

We have investigated the photodissociation dynamics of jet-cooled HOD via the $\widetilde{C}$ state around 124 nm using the high resolution Rydberg H(D)-atom tagging technique. The rotational-state-specific action spectrum shows five clearly resolved transition lines, and the corresponding total product translational energy distribution spectra for representative lines present the rovibrational state distributions of OH(X)/OD(X) and OH(A)/OD(A) products. Branching ratios between H+OD and D+OH channel of the five transitions for the $\widetilde{C}$-$\widetilde{X}$ transition have been estimated to be larger than 1, which means that the dissociation process of HOD favors the route to H+OD channel. The comparison between the ratios of $\widetilde{C}$-$\widetilde{X}$ transition with those of the $\widetilde{B}$-$\widetilde{X}$ and $\widetilde{A}$-$\widetilde{X}$ transitions shows that the isotopic branching ratio (OD/OH) is a strong function of the frequency of the dissociation photon. In addition, we have also determined the accurate OD bond dissociation energy of HOD to be 41751.3±5 cm^{-1}, which is the supplement of the dissociation energies of water and its isotopes.

V. ACKNOWLEDGMENTS

This work was supported by the Chinese Academy of Sciences, the Ministry of Science and Technology, and the National Natural Science Foundation of China.

[1] R. Schinke, *Photodissociation Dynamics*, 1st edn., Cambridge: Cambridge University, 11 (1993).
[2] B. P. Bonev and M. J. Mumma, Astrophys. J. **653**, 788 (2006).
[3] D. W. Hwang, X. F. Yang, and X. M. Yang, J. Chem. Phys. **110**, 4119 (1999).
[4] X. F. Yang, D. W. Hwang, J. J. Lin, and X. Yang, J. Chem. Phys. **113**, 10597 (2000).
[5] I. C. Lu, F. Y. Wang, K. J. Yuan, Y. Cheng, and X. M. Yang, J. Chem. Phys. **128**, 066101 (2008).
[6] R. N. Dixon, D. W. Huang, X. F. Yang, S. A. Harich, J. J. Lin, and X. Yang, Science **285**, 1249 (1999).
[7] S. A. Harich, D. W. Huang, X. F. Yang, J. J. Lin, X. M. Yang, and R. N. Dixon, J. Chem. Phys. **113**, 10073 (2000).
[8] S. A. Harich, X. F. Yang, D. W. Huang, J. J. Lin, X. M. Yang, and R. N. Dixon, J. Chem. Phys. **114**, 7830 (2001).
[9] S. A. Harich, X. F. Yang, X. M. Yang, and R. N. Dixon, Phys. Rev. Lett. **87**, 253201-1 (2001).
[10] S. A. Harich, X. F. Yang, X. M. Yang, R. van Harrevelt, and M. C. van Hemert, Phys. Rev. Lett. **87**, 263001-1 (2001).
[11] K. J. Yuan, L. N. Cheng, Y. Cheng, Q. Guo, D. X. Dai, and X. M. Yang, J. Chem. Phys. **131**, 074301 (2009).
[12] (a) M. N. R. Ashfold, J. M. Bayley, and R. N. Dixon, Can. J. Phys. **62**, 1806 (1984);
(b) M. N. R. Ashfold, J. M. Bayley, and R. N. Dixon, Chem. Phys. **84**, 35 (1984).
[13] H. H. Kuge and K. Kleinermanns, J. Chem. Phys. **90**, 46 (1989).
[14] K. J. Yuan, Y. Cheng, L. N. Cheng, Q. Guo, D. X. Dai, X. M. Yang, and R. N. Dixon, Proc. Natl. Acad. Sci. **105**, 19148 (2008).
[15] L. N. Cheng, K. J. Yuan, Y. Cheng, Q. Guo, X. M. Yang, and R. N. Dixon, Mol. Phys. **108**, 905 (2010).
[16] K. J. Yuan, Y. Cheng, L. Cheng, Q. Guo, D. Dai, X. Yang, and R. N. Dixon, J. Chem. Phys. **133**, 134301 (2010).
[17] Y. Cheng, L. Cheng, Q. Guo, K. Yuan, D. Dai, X. Wang, R. N. Dixon, and X. Yang, J. Chem. Phys. **133**, 034307 (2010).
[18] L. N. Cheng, K. J. Yuan, Y. Cheng, Q. Guo, T. Wang, D. X. Dai, X. M. Yang, and R. N. Dixon, J. Phys. Chem. A **115**, 1500 (2011).
[19] H. Akagi, H Fukazawa, K Yokoyama, and A. Yokoyama, J. Chem. Phys. **123**, 184305 (2005).
[20] M. Sarma, S. Adhikari, and M. K. Mishra, J. Chem. Phys. **127**, 024305 (2007).
[21] A. K. Tiwari, K. B. Møller, and N. E. Henriksen, Phys. Rev. A **78**, 065402 (2008).
[22] L. Schnieder, W. Meier, K. H. Welge, M. N. R. Ashfold, and C. Western, J. Chem. Phys. **92**, 7027 (1990).
[23] L. Schneider, K. Seekamp-Rahn, E. Wrede, and K. H. Welge, J. Chem. Phys. **107**, 6175 (1997).
[24] K. J. Yuan, L. N. Cheng, Y. Cheng, Q. Guo, D. X. Dai, and X. M. Yang, Rev. Sci. Instrum. **79**, 124101 (2008).
[25] J. P. Marangos, N. Shen, H. Ma, M. H. R. Hutchinson, and J. P. Connerade, J. Opt. Soc. Am. B **7**, 1254 (1990).
[26] W. Yi, J. Park, and J. Lee, Chem. Phys. Lett. **439**, 46 (2007).
[27] N. Shafer, S. Satyapal, and R. Bersohn, J. Chem. Phys. **90**, 6807 (1989).
[28] V. Engel and R. Schinke, J. Chem. Phys. **88**, 6831 (1988).

DOI:10.1088/1674-0068/24/02/129-133